Reference Ballistic Chronograph for Personal Armor Characterization[1]

Nicholas G. Paulter, Jr.
Donald R. Larson (corresponding author)
Office of Law Enforcement Standards
NIST
100 Bureau Drive
Gaithersburg, MD 20899-8102
Email: donald.larson@nist.gov
Fax: 301-948-0978

Abstract:
Ballistic armor is evaluated using a V_{50} parameter, which describes the velocity above which half the shots would be expected to perforate a given type of body armor. The lower the error and uncertainty in measuring the velocity of the bullet, the lower the uncertainty in establishing an accurate V_{50} value. Reproducibility between chronographs is also important for inter-laboratory comparisons of ballistic armor performance. We describe a ballistic chronograph designed to provide an estimate of bullet velocity with an associated uncertainty in the velocity measurement of less than $\pm$ 0.2 m/s, much lower than the errors and/or accuracies claimed by manufacturers of commercially available systems.

Keywords: ballistic chronograph, personal armor, pulse analysis, velocity, uncertainty.

1. Introduction

Ballistic chronographs are used to measure the velocity of projectiles (bullets). This is important to help in developing formulas for different gun powders and designing bullet shapes and gun components. For law enforcement and military applications, an even more important application is the assessment and characterization of ballistic armor ("bulletproof" vests). Our purpose for developing this chronograph was to address ballistic armor assessment.

Ballistic armor is commonly evaluated using two types of tests: perforation testing, where bullets are fired at a specified velocity to verify that the armor will not be perforated, and V_{50} testing, where bullets are fired at different velocities to estimate the velocity above which half the shots would be expected to perforate the body armor and below which half the shots would not be expected to perforate the armor. (A shot is an event where one bullet is fired.) Reduced error and uncertainty in measuring the velocity of the bullet leads to greater confidence that velocities meet specifications, and for V_{50} testing, reduces the uncertainty in the estimated V_{50} value. Reproducibility between chronographs is also very important for inter-laboratory comparisons of ballistic armor performance.

There have been several different technologies used for ballistic chronography. One popular type of chronograph uses radar technology and another uses light bars with opposing optical detectors. The radar device is a conventional Doppler radar, where the bullet velocity is determined by the frequency shift of the reflected radio frequency power from the

[1] Contribution of the National Institute of Standards and Technology; not subject to copyright in the United States.

approaching or receding bullet. The light bars with opposing optical detectors basically are frames with light emitters lining a top bar and optical detectors lining the bottom bar. Two such frames separated by a known distance are required. The bullet velocity is computed from the separation between the two frames and the time interval between the bullet blocking the light to an optical detector in the first frame to when it blocks the light to an optical detector in the second frame. Other technologies that have been used include ultra-high speed cameras and inductive sensors, essentially very high speed metal detectors.

The typical manufacturer-provided uncertainty for the velocity estimate is ± 1 %. For bullet velocities of 400 m/s (1312 ft/s), a ± 1 % uncertainty corresponds to ± 4 m/s (± 13 ft/s). This error may be adequate for characterization of ballistic armor, but since multiple chronographs give different measurement results, the performance of the chronographs must also be evaluated.

2. Measurement System

This measurement system was designed to provide an estimate of the projectile velocity with an associated uncertainty that is much lower than commercially available systems.

The ballistic chronograph comprises three components: the light source, the head, and the light detection component (Fig. 1). The chronograph head is mounted directly to the universal receiver or barrel of the firearm using appropriate adapters (not shown). The light source and light detection components are located remote to the head and are connected to it using optical fiber cables of equal lengths.

The light source is a fiber coupled, cw, semiconductor laser operating in the near IR (wavelength is 1550 nm) with an optical output power that can easily saturate the response of all three optical detectors used in the light detection component. The single-mode fiber coupled output of the laser is split into three other fibers so that each fiber carries nominally equal power. Each of these fibers is then connected to a separate fiber pigtailed collimator that is mounted in the head. The collimators are FC-connectorized for easy take-down and assembly of the ballistic chronograph, and for ease of repair. Several of the popular fiber optic connectors are mostly plastic. The metal/ceramic construction of the FC connectors used here is assumed to add to the ruggedness of the system.

The chronograph head consists of several mechanical and optical components. The optical components are the fiber pigtailed collimators already mentioned and collectors, arranged in pairs such that the output of the collimator faces the input of the collector with their optical axes nominally collinear. The commercially available collector is a small lens mounted in an FC connector. There are three collimator/collector pairs; each pair is mounted in a separate aluminum mounting flange which establishes the spacing between each collimator and its associated collector. Each of these flanges is attached to the other using fixed-length, Invar posts. The center-to-center spacing between beam centers of each pair in the assembled head is nominally 8 cm. The light detection component includes the light collectors, the optical detectors, and the waveform recorder (for which we use a real-time digital oscilloscope). The collectors and optical detectors are connected by 550 μm-core multimode fiber, which was selected to maximize light collection and minimize sensitivity to misalignment and shock. These fibers are connected to amplified indium-gallium-arsenide (InGaAs) photodiodes having a 3 dB attenuation bandwidth of 125 MHz and output impedance of 50 Ω. These three

optical detectors are each connected to a different input channel of the oscilloscope. The oscilloscope has a 3 dB attenuation bandwidth of 350 MHz.

3. Operation

In operation, the bullet blocks each of the three laser beams in sequence and in response, the three amplified optical detectors each output a negative going electrical pulse waveform. These three pulse waveforms are captured using three channels of the oscilloscope. The first electrical pulse is also used to trigger the oscilloscope. Along with the other two pulse-like waveforms created when the bullet blocked the other succeeding two laser beams, these pulse-like waveforms are acquired and analyzed. The interval between the three pulses, together with the knowledge of the physical spacing of the laser beams is used to calculate the velocity of the bullet. Figure 2 depicts the waveforms acquired with the oscilloscope and transferred to a computer for analysis. Each waveform typically consists of 10^4 data points.

4. Measurement Results

The reference ballistic chronograph was tested using an ANSI/SAAMI test barrel mounted to a universal receiver [1]. Several different bullet shapes were used, 44 cal. magnum semi-wadcutters with a gas check, 357 cal. jacketed soft point, 9 mm hollow point and 9 mm full metal jacket, round nose. Velocity estimates were compared with estimates from two or three commercially available ballistic chronographs, two of the same model from one manufacturer and one from another manufacturer. All three are optically based and similar to the reference ballistic chronograph; they sense the change in light level as the bullet passes between the optical light source and the optical detector. Table 1 contains a few representative measurement results; B1 and B2 are two commercially available ballistic chronographs from the same manufacturer (same model) and A1 is a commercially available ballistic chronograph from another manufacturer.

Table 1.

Velocity (m/s)/ Bullet	Reference Ballistic Chrono	A1	B1	B2
9 mm round	444.0	444.1	440	440
9 mm round	408.7	408.5	406	406
9 mm hollow point	361.4	n/a	365	365
9 mm hollow point	382.2	n/a	383	380
357 cal.	535.9	535.8	531	531
44 Mag.	466.7	n/a	464	463

The chronographs were arranged in a serial fashion, the reference ballistic chronograph was mounted on the muzzle, chronographs A1, B1 and B2 were located approximately 1.6 m, 2.0 m, and 2.1 m from the muzzle respectively. All testing occurred in the OLES Ballistics Range, an indoor facility located at NIST. Please note that the data in Table 1 are not compensated for possible velocity variations of the bullet due to drag or other factors.

5. Uncertainty analysis

The bullet velocity is computed by dividing the distance traveled by the time it took for the bullet to travel that distance. The distance, *d*, is the separation between the axes of the laser beams from two adjacent collimator/collector pairs. The travel time, *t*, of the bullet is

determined from the oscilloscope waveforms. The velocity, s, of the bullet is given in units of length (typically meters) per unit of time (seconds):

$$s = \frac{d}{t}. \tag{1}$$

The uncertainty, u_s, in the velocity estimate is:

$$u_s = \sqrt{\frac{u_d^2}{t^2} + \frac{u_t^2 d^2}{t^4} + u_r^2}, \tag{2}$$

where u_d is the uncertainty in d , u_t is the uncertainty in t, and u_r is the variability in the velocity estimates. The contributors to the uncertainties u_d, u_t, and u_r are considered in the following subsections.

5.1. Uncertainty, u_d, in distance traveled

The contributions to the uncertainty, u_d , in the distance, d, are considered in the following subsections. The distance between the optical beams is measured using a knife edge attached to a stepping motor driven stage and a digital voltmeter connected to the optical detectors. The knife edge is passed through each of the three optical beams in a path that is nominally collinear with that of the bullet. As the knife edge passes through the optical beam, the laser energy coupled into the optical detector decreases and is eventually blocked completely. The output signal of the optical detector tracks this optical input and it is this step-like output signal that is monitored by the voltmeter.

The transition region of the step-like waveform contains information on the beam diameter at the location where the knife edge passes through it. The beam diameter can be determined by taking the derivative of the step-like waveforms that were obtained when measuring the distance between collimator/collector pairs and then computing the e^{-2} points of the resultant Gaussian-like waveform. The beams' diameters, measured near the center of the head, were nominally 500 μm and the standard deviation of the beam diameter measurements were nominally ± 0.6 μm.

5.1.1. Uncertainty in distance between optical beams

Since there are three collimator/collector pairs, we obtain three $V(x_i)$ waveforms, one for each of the collimator/collector pairs. The distance, $d_{2\text{-}1}$, between the laser beam propagating between the first collimator/collector pair and the laser beam propagating between second collimator/collector pairs is computed using:

$$d_{2-1} = p_2 - p_1, \tag{3}$$

where p_1 and p_2 are the computed positions of the beam centers for the first and second collimator/collector pair respectively. The beam center is the 50 % reference level position of the step-like waveform. Since each of these data pair sets is acquired M times, we can compute the mean distance for $d_{2\text{-}1}$ (as an example) using:

$$\bar{d}_{2-1} = \frac{1}{M}\sum_{m=1}^{M} d_{2-1,m} \tag{4}$$

and its standard deviation, $\sigma_{d,2\text{-}1}$, using:

$$\sigma_{d,2-1} = \sqrt{\frac{1}{M}\sum_{m=1}^{M}\left(\bar{d}_{2-1} - d_{2-1,m}\right)^2}. \tag{5}$$

A similar computation is done for $d_{3\text{-}2}$ using p_2 and p_3.

5.1.2. Uncertainty in beam position

The distance between the laser beams is dependent on the estimate of the position of the laser beam centers, p_1, p_2, and p_3. As previously stated, p_1 is the value of the 50 % reference level position of the first laser beam. u_{p1} is the uncertainty in the position value for p_1 (which includes interpolation effects). u_{p2} is the uncertainty in the position value for p_2 and u_{pos} is the uncertainty in positioning of and/or in the reading of the position of the stepping motor translation stage. The multiplier of 2 appears in front of u_{pos} because two separate positions are used to determine the distance. We have previously calculated the uncertainty [2] in determining reference level instants (see ref. 3, IEEE Std 181-2003, for description of terms), which are identical for computational purposes to the position values (p_i, i = 1, 2, 3) described here. Using this analysis, we find the uncertainties, u_{p1}, u_{p2}, and u_{p3} to each be ± 5 μm. The uncertainty, u_{pos}, in positioning the stepping motor stage, estimated from the manufacturer's specifications, is less than ± 0.5 μm.

5.1.3. Uncertainty in distance estimate due to thermal expansion of the head

The distance between laser beams is nominally 8 cm, 2 cm of which is contributed by the aluminum collimator/collector mounting flange, and 6 cm of which is contributed by invar posts. Thermal expansion or contraction of these materials will cause changes in the distance between the laser beams. Although the temperature of the NIST Ballistics Range is well controlled, any temperature variations will result in small differences in velocity estimates. Assuming a difference in ambient temperature of 4 ˚C between calibration of the distance between laser beams and a bullet velocity measurement, $u_{d(T)}$, the uncertainty in the laser beam separation for this head configuration is ± 2.2 μm. The use of invar posts helps minimize this variation.

5.1.4. Combined uncertainty in the distance estimate

The combined uncertainty in the distance between beam centers is computed using:

$$u_{d,2-1} = \sqrt{\sigma_{d,2-1}^2 + u_{p_1}^2 + u_{p_2}^2 + 2u_{pos}^2 + u_{d(T)}^2}\,, \qquad (6)$$

where the contributors to $u_{d,2\text{-}1}$ and their values are:

$\sigma_{d,2\text{-}1}$ = ± 4.1 μm,
u_{p1} = ± 5 μm,
u_{p2} = ± 5 μm,
u_{pos} = ± 0.5 μm, and
$u_{d(T)}$ = ± 2.2 μm.

The value of $u_{d,2\text{-}1}$ for typical measurement results and conditions, such as for the waveforms shown in Fig. 2, is ± 8.5 μm. The value of $u_{d,3\text{-}2}$ is the same.

5.2. Uncertainty in the time for the distance traveled, u_t.

The time corresponding to the distance traveled by the bullet is computed by taking the difference between the appropriate reference level instant of the waveforms acquired from each of the three channels to which an optical detector is attached. We select the 50 % reference level instant because the estimate of the 50 % reference level is less affected by

noise than other reference levels. Noise is important with these waveforms because no averaging is performed (these are single-shot measurements). Before developing a mathematical expression that describes u_t, we will first describe the factors that can contribute to the uncertainty in t.

5.2.1. Chronograph-head-related factors contributing to u_t.

All non-ideal mechanical and geometrical factors can contribute to u_t. These factors include:

1. Bullet trajectory is not coaxial with the axis of the head.
2. Bullet trajectory is changing (spiraling, wobbling, monotonic displacement with distance) as it passes through head.
3. Bullet is not normal to the beams.
4. Optical beam profile is different amongst the beams.
5. Optical beams are not normal to head axis.
6. Recoil changes effective distance between sequential collimator/collector pairs.

Although it is possible to derive mathematical expressions describing these contributors, it is not necessary. Information on these effects is contained, redundantly, in the acquired time-domain waveforms. For example, if the bullet, for whatever reason, does not provide the same profile to each laser beam as it passes through the three beams, three effects will be observed: variation in the values of the first transition durations, [3] variations in the values of the second transition durations, and variations in values of the pulse durations. Any one to all of the six reasons listed above can cause this difference. The first transition corresponds to the nose of the bullet (which may be pointed or flat) and the second transition duration to the tail of the bullet (which is almost always nominally flat), the variation in the first transition duration values will be more sensitive to the mechanical and geometric factors than the second transition duration. However, in order to minimize the effects of blow-by, the optical detectors are operated in saturation by increasing the optical power from the laser. Consequently, the duration of the first transition is significantly longer than the second transition duration. The pulse duration is also increased by operating the optical detectors in saturation. This masks some of the bullet shape and trajectory effects on the first transition duration and on the pulse duration. However, the variation in the second transition durations should still indicate these effects. Since the second transition duration is also the shortest, it is used to calculate the velocity and u_t. The mean of these transition durations is given by:

$$\overline{\tau_i} = \frac{1}{N}\sum_{n=1}^{N} \tau_{i,n} \qquad (7)$$

where $\tau_{i,n}$ is the transition duration of the waveform taken from each of the three channels of the oscilloscope, i is the transition duration index (i=1 being the first or negative transition and i=2 is the second or positive transition), and the n subscript denotes one of the three oscilloscope channels, which corresponds to one of the collimator/collector pairs, and $N = 3$. The standard deviation for the mean transition duration values is:

$$\sigma_{\tau_i} = \sqrt{\frac{1}{N}\sum_{n=1}^{N}\left(\overline{\tau_i} - \tau_{i,n}\right)^2}, \qquad (8)$$

We have previously developed an analysis to determine the uncertainty in transition duration values [2] that includes the standard deviation, instrument effects, computational effects, sampling interval size, etc. However, the uncertainties due to these other effects are less than 1% of the standard deviation in the transition duration values and were ignored.

5.2.2. Oscilloscope timebase calibration

The oscilloscope timebase must be calibrated to ensure the sampling interval is known and uniform. If not, these errors may have to be corrected and/or appropriate uncertainties attributed to the temporal information of the waveforms. The timebase error, $u_{\Delta t}$, was measured using known sinewave signals in a method described in [4]. The linear part of the timebase error can be easily corrected by correcting the value of the sampling interval. The variation between the linear fit to the timebase values and the actual measured values is used to compute $u_{\Delta t}$. For the oscilloscope used in this study, $u_{\Delta t}$ was determined to be ± 0.7 ns.

5.2.3. Differential delays between chronograph head and initial instants of waveforms

This delay has three primary sources: differing lengths of fiber optic cable running between the chronograph head and the optical detector, different operating delays of the optical detectors, and skew between channels of the oscilloscope. The transition duration of the optical pulses generated will be about 0.4 μs or more, the length of the multimode optical fiber between the head and the detectors is about 10 m, and the line width of the laser source is less than 0.1 MHz. Consequently, pulse distortion resulting from chromatic and modal dispersion would be less than about 0.4 ns and very similar for each signal path; it is neglected here. Differences in optical fiber cable lengths as much as ± 0.5 m will introduce differential time delay of about ± 2.5 ns, assuming a nominal propagation velocity of 2×10^8 m/s. This and the other contributors can be measured simultaneously using the measurement set up in Fig. 3. A mechanical light chopper is inserted before the three way optical fiber splitter and provides three almost simultaneously generated and nearly identical optical pulses to each of the three collectors and corresponding optical detector and oscilloscope channels. We measured a differential delay of ± 10 ns from the three oscilloscope channels. Although this value includes differences in signal path from the laser to the collimators, differences that would not affect the measurement of bullet velocity, it is used as an estimate of u_{Δ}, the uncertainty due to differential delays.

5.2.4. Combined uncertainty in the time estimate

The uncertainty in the time estimate for the distance traveled is given by:

$$u_t = \sqrt{\sigma_{\tau_2}^2 + u_{\Delta t}^2 + u_{\Delta}^2}, \qquad (9)$$

where $\sigma_{\tau 2}$ is the uncertainty in the second transition durations of the pulses. $u_{\Delta t}$ is the uncertainty in the oscilloscope timebase and u_{Δ} is the uncertainty due to the differential delay. Typical values for the contributors to u_t are:

$\sigma_{\tau 2} = \pm 24.6$ ns,
$u_{\Delta t} = \pm 0.7$ ns, and
$u_{\Delta} = \pm 10$ ns.

The value of u_t for typical measurement results and conditions, such as for the waveforms shown in Fig. 2, is 26.6 ns.

5.3. Velocity uncertainty, u_s

The velocity is determined using a linear least squares fit to the three distance-time data points. The velocity is the reciprocal of the slope of the fitted line. The uncertainty, u_r, due to

the variability of this velocity determination is found using the standard error of the slope and is given by:

$$u_r = \sqrt{u_e^2(y) / y^4}, \qquad (10)$$

where u_e is the standard error of the slope y. A typical value for u_r is 0.07 m/s.

The above uncertainty estimates for distance, time and velocity are combined using the root-sum-of-squares method as indicated in equation 2, reproduced here.

$$u_s = \sqrt{\frac{u_d^2}{t^2} + \frac{u_t^2 d^2}{t^4} + u_r^2}, \qquad (2)$$

The effective degrees of freedom is estimated using the Welch-Satterthwaite formula, and the coverage factor is found from the t-distribution for a 95 % level of confidence [5]. The expanded uncertainty is the product of the coverage factor (2.0 for 95 % level of confidence) and the combined uncertainty [5]. For the waveforms shown in Figure 2 and the measurement conditions, we get s = 361.4 m/s ± 0.2 m/s. The expanded uncertainty is about 0.05 % of the velocity, compared to about 1 % for commercial ballistic chronographs.

6. Conclusion

By using a waveform recorder (oscilloscope) and pulse analysis techniques, a ballistic chronograph can be developed that provides velocity estimates with at least an order of magnitude lower uncertainty than commercially available ballistic chronographs. Because of this low uncertainty, this chronograph can be used as a reference to calibrate and/or characterize the performance of commercially-available chronographs.

Acknowledgments

We would like to thank Nathaniel Waters for providing access to and running the firing range and to Kirk Rice for providing information on performance requirements and editorial assistance. We also acknowledge Dr. William Guthrie for assistance with the uncertainty analysis.

References

1. ANSI/SAAMI Z299.3-1993 “Voluntary Industry Standards for Pressure and Velocity of Centerfire Pistol and Revolver Ammunition for the Use of Commercial Manufacturers,” Sporting Arms and Ammunition Manufacturers’ Institute, 11 Mile Hill Road, Newtown, CT 06470.

2. N.G. Paulter and D.R. Larson, “Pulse parameter uncertainty analysis,” Metrologia, Vo. 29, pp. 143-155, 2002.

3. IEEE Std. 181-2003, “Standard on Transitions, Pulses, and Related Waveforms,” Institute of Electrical and Electronic Engineers, 445 Hoes Lane, Piscataway, NJ 08855, USA.

4. G.N. Stenbakken and J.P. Deyst, “Time-base nonlinearity determination using iterated sine-fit analysis,” IEEE Trans. Instrum. Meas.,Vol. 47, pp. 1056 to 1061, October 1998.

5. “ISO Guide to the Expression of Uncertainty in Measurement,” ISO, Geneva (1993).

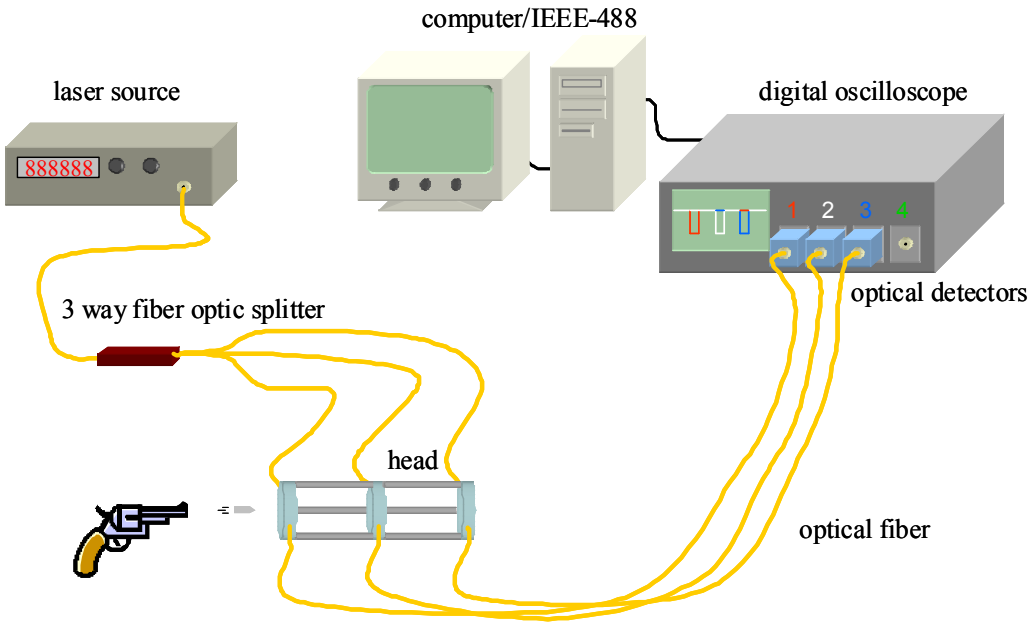

Figure 1. Reference Ballistic Chronograph

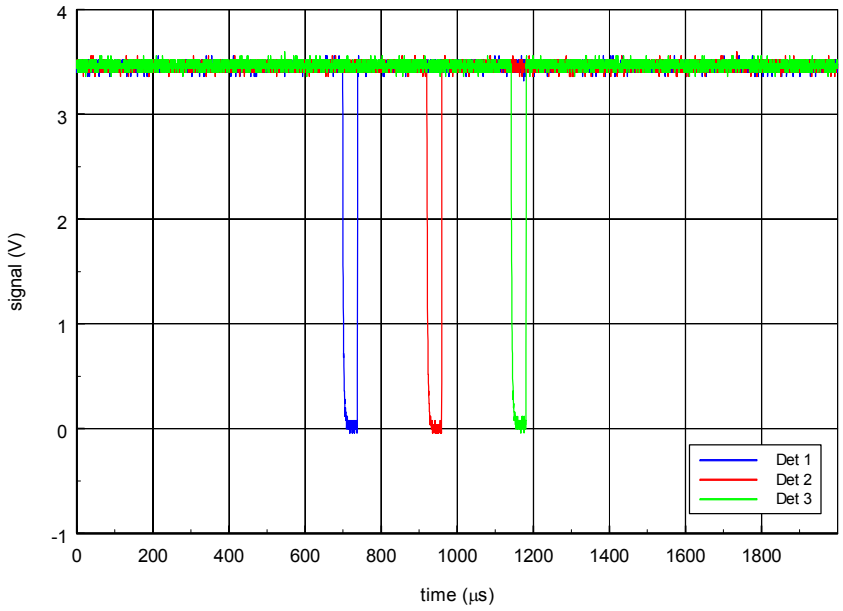

Figure 2. Three waveforms acquired by oscilloscope.

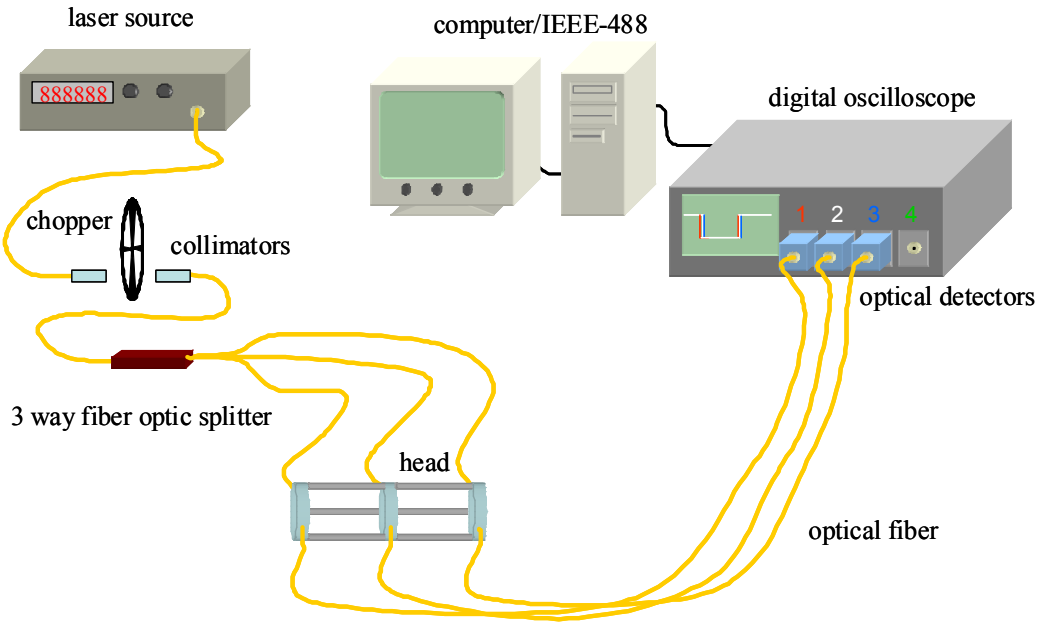

Figure 3. Chronograph with chopper and fiber optic collimators.